Imperfect Fabry-Perot resonators

Klaassen, T.

CHAPTER 2

Characterization of scattering in an optical resonator

Roughness-induced scattering affects the performance of a resonator. We study the scattering of a single mirror first, and compare this result with the losses of a resonator, comprising two mirrors. Besides some standard tools to characterize the losses, a new method based on the spectrally averaged transmission is introduced.

2.1 Introduction

Fabry-Perot resonators in textbooks are assumed to have ideal, lossless and perfectly smooth mirrors; however, those used in experiments are often far from ideal and have deformations on various length scales. In Bennett *et al.* [18], three regimes of deformations are defined based on the size of the roughness features (denoted between brackets): *surface roughness* (< 0.1 mm), producing light scattering, *waviness* ($0.1 - 10$ mm) contributing to the small angle scattering, and *surface figure* (> 10 mm) or deviations from the ideal geometrical shape, deforming the modes in the resonator. All three types of roughness can drastically affect the behavior of the resonator dynamics as will be pointed out in the following Chapters of this thesis. In this Chapter, we will focus on scatter. In Chapter 4, 5, and 6 we will consider surface figure.

The surface quality of mirrors is of crucial importance in a field like cavity QED [4] and applications such as ring-laser gyroscopes and gravitational wave detectors, like LIGO [7], VIRGO [8] and TAMA [9]. For all these fields and applications, the roughness-induced scatter limits the ultimate performance. Specifically, in cavity QED-experiments the coupling between field and atom gets worse [22], whereas for ring-laser gyroscopes the scatter couples the propagating and counter-propagating modes and thus lowers the sensitivity [23]. Light scattered out of the lowest order mode of a gravitational wave detector reduces the fringe contrast and thus the performance [24–27]. State-of-the-art mirrors with ditto coatings have a loss (both absorption and scatter) in the order of 10^{-6} per reflection and a surface roughness (RMS) of 0.1 nm [22, 26, 28].

In this Chapter, we will visualize and demonstrate the amount and distribution of the scatter in a resonator. The mirrors used in these experiments have a diameter of 5 cm, and a radius of curvature $R = 50$ cm. The measured transmittance of the mirror is $T = 4.1 \times 10^{-4}$ at the central reflecting wavelength of 532 nm. The substrate and multilayer coating have a very small absorption loss as compared to the scatter loss; this absorption loss will be neglected (see *e.g.*, [22]). The mirrors described in this Chapter are typical for those used in most experiments of this thesis.

In Section 2.2, the losses of a single mirror are characterized, while Section 2.3 and Section 2.4 discuss the effect of loss in a two-mirror Fabry-Perot cavity. Whereas most loss-measurements performed on a Fabry-Perot are based on the observed resonance linewidth, we will show that similar information can be obtained from a new method that is based on a measurement of the spectrally-averaged transmission. This method turns out to be simple and accurate. Conceptually, the most logical way to measure the spectrally *averaged* transmission is to use *incoherent* illumination, *e.g.*, by using a LED: this measurement has been performed first. Then we demonstrate that the average transmission $\langle T(\phi) \rangle$ (ϕ is round-trip phase) of a *coherently* illuminated resonator gives identical results. Section 2.4 describes the resonator losses as found from the, widely used, finesse and cavity ring-down. We conclude with a comparison and discussion of the various methods in Section 2.5.

2.2 Single-mirror scattering

The amount and distribution of the roughness-induced scatter of a single mirror can be visualized and quantified with a setup as shown in Fig. 2.1. A CW-single-frequency-laser (IN-

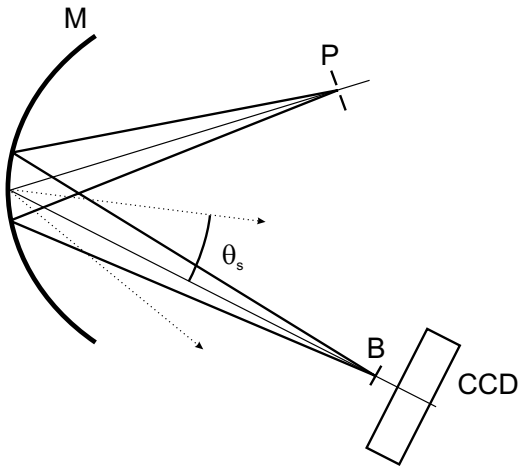

Figure 2.1: *Overview of the setup for measuring the scatter of a single mirror, M. The mirror is illuminated by light diffracted on a pinhole P. The dotted arrows indicate light scattered at the mirror under an angle θ_s. The distances between pinhole and mirror (PM) and mirror and image of the pinhole (MB) are 36 cm and 81 cm, respectively. The angle between both arms $\angle PMB$ is* 12°*. The image is blocked, B, to prevent overexposure of the CCD.*

NOLIGHT Prometheus) at a wavelength $\lambda = 532$ nm illuminates a pinhole *P* with a diameter of 200 µm. The pinhole is imaged by the concave mirror under study. In the image plane of the pinhole, the image is blocked to prevent the linear CCD-camera (Apogee Alta U1) from overexposure by the on-axis beam. As the sensitive area of the CCD is only 6.9×4.1 mm^2, we use a patchwork of images on several lateral positions, to obtain the scattering profile over a larger angular range. This results in an image as shown in Fig. 2.2. The center shows the obscuration blocking the on-axis beam; the speckles in the picture result from light scattered out of the on-axis beam due to roughness on the mirror surface. The effect of scatter is clearly visible although the intensity in the central spot and the scattered light differ by $7-8$ orders of magnitude. The speckles in Fig. 2.2 result from interferences of the spatially-coherent contributions from different parts of the mirror. Taking a closer look at the speckles, we see the rotational symmetry of the scatter pattern. Furthermore, it turns out that all speckles have roughly the same size, but what determines this size? To answer this question we have to consider that the speckle is Fourier-related to the illuminated area on the mirror and that this area is again (inversely) Fourier related to the pinhole. This means that the speckles are in a way just scaled and randomly displaced images of the pinhole. Statistics on the size of the speckles do indeed show that the speckles have approximately the size of the pinhole scaled by the imaging-magnification.

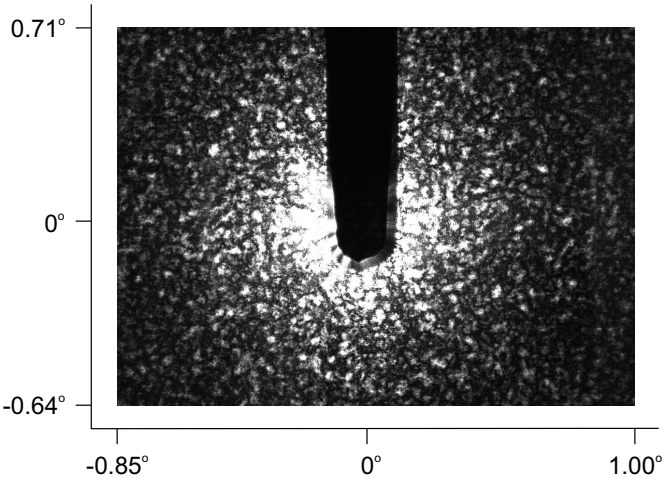

Figure 2.2: *Figure consisting out of 25 CCD images of the scatter from a single mirror. In the center an obscuration blocks the direct beam. The speckles are formed by scatter due to surface roughness of the mirror.*

The speckle pattern is not caused or influenced by edge-diffraction of the mirror as the diameter of the spot (Airy-disk) on the mirror (at $L_1 = 36$ cm away from the pinhole) is small ($1.22\lambda L_1/D \approx 2$ mm) as compared to the size of the mirror. Furthermore, the spot on the mirror is also small as compared to the relevant dimensions of Fig. 2.2, so we can neglect the finite size of the illuminated area and treat it approximately as a point scatterer in our analysis of the angle dependence of the scatter.

The standard way to quantify the distribution and the total amount of scatter of a mirror is expressed by the so-called Bidirectional Reflectance Distribution Function (BRDF) and the Total Integrated Scatter (TIS) [18, 29], respectively. The BRDF is defined as

$$\mathrm{BRDF} = \frac{1}{P_0}\frac{dP}{d\Omega\cos\theta_s}\,, \tag{2.1}$$

where dP is the optical power scattered into a projected solid angle $d\Omega\cos\theta_s$, θ_s is the scattering angle, and P_0 is the incident energy from the surface. The $\cos\theta_s$-term is a correction to adjust the illuminated area on the mirror to its apparent size when viewed from the scatter direction. When the BRDF is integrated over the solid angle, where θ_s ranges from 0 to $\pi/2$ and ϕ from 0 to 2π, the TIS is found. A correction for the $\cos\theta$-term is made in this integration. The connection between the TIS and the RMS surface roughness σ, is given by [29]

$$\mathrm{TIS} = \left(\frac{4\pi\sigma}{\lambda}\right)^2\,, \tag{2.2}$$

assuming that the light is normally incident on the surface. As the scatter was observed to be nicely rotational symmetric, we can use data from one radial direction only. To calculate the BRDF over a larger angular range than found in Fig. 2.2 some additional images were made. To limit the fluctuations in the offset (to ~ 10 units on the 2^{16} scale of the 16 bit camera)

we average on every position over 10 images. Furthermore, to get rid of the speckles, the image is averaged over many vertical pixel lines. The resulting BRDF is shown in Fig. 2.3, where θ_s ranges from 0.14° to 7.6°. The black line fits the calculated data with BRDF$= 0.036 \times \theta_s^{-1.33}$. Mirror surfaces which can be described by such a simple power law are named fractal surfaces [29, 30]. Now that we know the distribution of the scatter, we can also calculate the TIS, by integration of the BRDF as found from the fit. The resulting TIS is 1.6×10^{-3}, half of which lies within the θ_s-range of $0 - 20^\circ$. So, for every bounce on the mirrors, a fraction 1.6×10^{-3} of the light is scattered out of the specular direction. This estimate is of course not very accurate as it is found via extrapolation outside the measured θ_s-range.

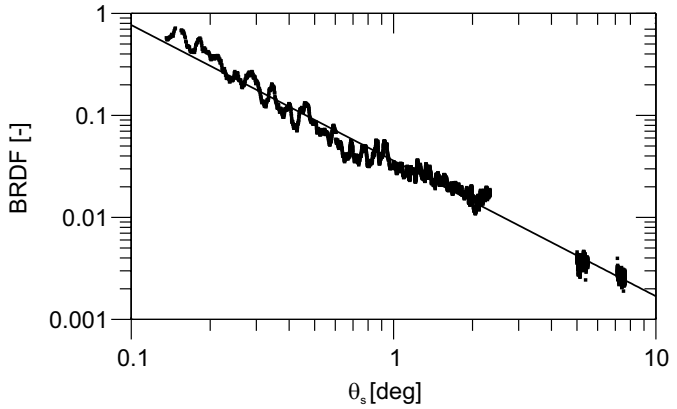

Figure 2.3: *The BRDF for θ_s from 0.14° to 7.6°. The black dots are the BRDF points calculated from similar measurements as shown in Fig. 2.2 and the black line is a fit of the data.*

A ratio that describes which part of the total light escapes the resonator via transmittance of the mirror is the resonator efficiency,

$$\eta = T/(A+T)\,, \tag{2.3}$$

where A is scatter (absorption can be neglected) and T the transmission. The mirror under study has $A = \text{TIS} = 1.6 \times 10^{-3}$ and $T = 4.1 \times 10^{-4}$, which results in $\eta = 20$ %. The rest of the light, roughly 80 %, leaves the resonator via scattering.

Substituting the thus calculated TIS in Eq. 2.2, results in a surface roughness $\sigma = 1.7$ nm. Measurements performed with a (WYKO RST-500) interferometer [31], however, gave a roughness of only $\sigma = 0.4$ nm. This huge difference might result from the wavelength dependence of the multi-layer coating, which comprises 14 pairs of alternating high and low refractive-index $\lambda/4$-layers (at $\lambda = 532$ nm). While our scattering measurement is performed at the design wavelength of 532 nm, the WYKO beam profiler, however, works at a wavelength of 633 nm. At this wavelength, the light penetrates the stack of layers much deeper than at 532 nm. It is not completely understood how this affects the comparison.

Similar experiments to determine the surface roughness have been done by Jakobs [32], Bruno [33], and Elson [34]. They measure the surface roughness of the top-layer with an

AFM and a stylus, out of which the scattering of the multi-layer system is calculated. As the phase relations between individual layers are unknown the calculations can only be performed for two extreme regimes, one where the roughnesses of the consecutive interfaces are fully correlated and the other where they are fully uncorrelated. The mentioned papers perform both calculations.

2.3 Resonator losses

The performance of a Fabry-Perot is generally described in terms of its resonance linewidth (in relation to the free spectral range). Not many people study the peak transmission and hardly anyone looks at the spectrally-integrated or averaged transmission. We will show that the resonator efficiency η can also be determined both from the average transmission under incoherent illumination, as well as from the average transmission of a coherently illuminated resonator $\langle T(\phi)\rangle$ when scanning the length of the Fabry-Perot.

The transmission of a resonator as a function of the single pass phase is [1]

$$T(\phi) = \frac{I_T(\phi)}{I_i} = \Big(\frac{T}{T+A}\Big)^2 \frac{1}{1+\big(\frac{2F}{\pi}\big)^2 \sin\phi^2}\,, \tag{2.4}$$

where F is the cavity finesse. The maximum peak transmission of the resonator is found for $\phi = 0$

$$T(0) = \frac{I_T(0)}{I_i} = \Big(\frac{T}{T+A}\Big)^2 = \eta^2\,. \tag{2.5}$$

The spectrally-averaged transmission, on which we will elaborate, is given by

$$\langle T(\phi)\rangle = \frac{\langle I_T(\phi)\rangle}{I_i} = \frac{T^2}{2(T+A)} = \tfrac{1}{2}T\eta\,, \tag{2.6}$$

where the relation $\langle[1+(\frac{2F}{\pi})^2\sin\phi^2]^{-1}\rangle = \pi/2F = (A+T)/2$ is used ($F^2 \gg 1$). The efficiency η defines how much of the light inside the resonator, leaves via transmission of the mirrors, the rest being scattered and absorbed. Taking into account that TI_i (see Fig. 2.4) defines how much light enters the resonator via the first mirror, Eq. 2.6 can also be rewritten as $\langle I_T(\phi)\rangle = \frac{T}{2(T+A)}TI_i = \frac{1}{2}\eta TI_i$.

2.3.1 Spectrally incoherent input beam

A LED, with a central wavelength $\lambda = 525$ nm and a spectral width of 36 nm (FWHM), is used for incoherent illumination of the Fabry-Perot. The mirrors of the resonator are identical to those used in Section 2.2. The cavity length is approximately 10 cm and the cavity is operated far from (lower-order) frequency-degenerate points (see Chapter 5). To operate the resonator at the same wavelength as with a coherent light source ($\lambda = 532.0$ nm), a spectral filter ($\lambda = 532.0$ nm, $\Delta\lambda_{\mathrm{FWHM}} = 3.5$ nm) is placed in front of the LED.

For a proper performance of the experiment, it is important to convert the highly-diverging light coming out of the LED into a more or less parallel beam. We want the light to remain paraxial inside the resonator even after multiple round-trips. This is done in two steps, where

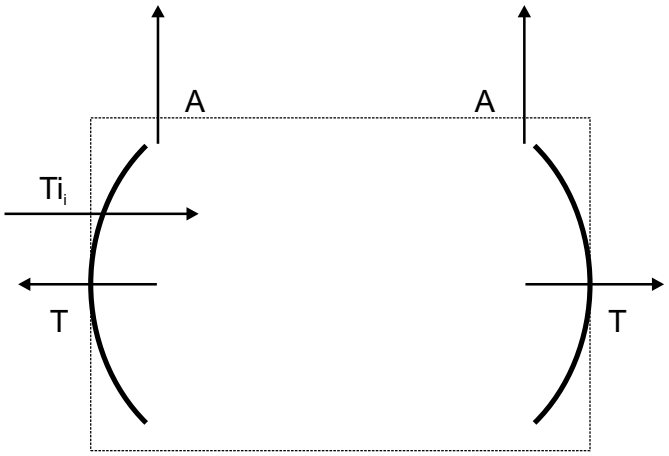

Figure 2.4: *Conservation of energy for an optical resonator requires that of the trapped light a fraction $T/(2T+2A) = \frac{1}{2}\eta$ is transmitted (coupled out) through each of the mirrors.*

first an enlarged image of the LED is made on a diaphragm (5 mm diameter) and a homogeneous part of this image is cut out. To improve the parallelism of the beam a second diaphragm (5 mm diameter) is placed 50 cm behind the first one, just in front of the resonator. The diameter of the diaphragms is chosen such that the diameter of the beam is smaller than of the detector (8 mm).

The power of the LED is roughly 1 mW, whereas the irradiance behind the mirrors falling onto the detector is sub-nW. To measure reliably at these low output powers, a photomultiplier (HAMAMATSU 5783-01) is used in combination with a chopper and a lock-in amplifier. The transmittance of the front mirror of the resonator, which we have measured first, is $T = (4.0 \pm 0.1) \times 10^{-4}$. This transmission is in nice agreement with the coherent measurement to be discussed in Section 2.3.2. Next, the transmittance behind the resonator (two mirrors) is measured, resulting in an efficiency of $\eta = (23.6 \pm 0.1)\%$. This means that roughly 75 % of the light inside the resonator is lost by scattering or absorption.

Finally, we also wanted to check whether the scatter losses (A-channel in Fig. 2.4) are as strong as would be expected from the (single mirror) BRDF-measurement, described in Section 2.2. For this purpose, the detector is moved from behind the resonator to the side of the resonator where it looks under an angle of 50° inside the resonator to the end mirror. The ratio of the integrated scatter (IS), measured by the detector at this position, divided by the measured scatter losses deduced from the area-integrated spectra (A-channel) is 5.9×10^{-3}. We can calculate a similar ratio from the single mirror BRDF in Section 2.2, as follows. The detector subtends a solid angle of $\Delta\Omega = 6 \times 10^{-2}$ sr at $\theta_s = 50°$. The integrated scatter (IS) is found from extrapolation of the measured BRDF to 50° and integration over the mentioned solid angle $\Delta\Omega$, which results in the ratio IS/TIS$= 6.8 \times 10^{-3}$. This ratio is in nice agreement with the measurement and confirms that the scatter strength as deduced from a two-mirror resonator is identical to that measured on a single mirror.

2.3.2 Spectrally coherent input beam

In the next experiment, the resonator is illuminated coherently by a laser (INNOLIGHT Prometheus) at 532 nm, where the beam is mode-matched to the resonator. The length of the resonator is scanned over a few λ with a piezo (PI P-753.1) to obtain the transmission spectrum. The resonances in the transmission (and reflection) spectrum depend on the phase ϕ, determined by λ, L and R. To be able to use the power arguments made in the beginning of this Section, the transmitted power is spectrally averaged over one free spectral range. Doing so, the phase is averaged out.

We know from the previous experiments that scattering losses are approximately $3-5$ times as strong as the transmission of the mirrors. A natural hypothesis is that the scattered light might be "trapped" inside the resonator in the form of (very) high-order modes and thus found in the "floor" of the Fabry-Perot spectrum, *i.e.*, between the resonances. Assuming a finesse of 1000 and a resonance voltage of 1 V on the detector, requires that a floor in the spectrum of 1 mV or less needs to be resolved. To do so, we used a 14-bit digitizer (National Instruments PCI-5911). To resolve the resonances also in the *horizontal* direction, the digitizer is operated at 5×10^6 samples/s. Fig. 2.5 shows the spectrum measured on two vertical scales (two detector amplifications); one to measure the dominant resonances in the spectrum and the other to measure the less prominent resonances and the floor properly. A lens is placed behind the resonator to catch all the light transmitted through the end mirror.

The first result of our measurement is that the floor, if it exists, is smaller than the noise level 0.02 mV, $T_{\text{floor}}/T_{\text{peak}} < 2 \times 10^{-5}$, which demonstrates that the scattered light is *not* found in the spectrum and is thus apparently *not* trapped inside the resonator. Furthermore, we found that the summed transmission on both measurement scales yields an efficiency of $\eta = (20 \pm 2)$ %. We thus find again that only 20 % of the light is transmitted through the mirror, while 80 % escapes via scatter. Of the transmitted intensity roughly 60 % is found in the single prominent resonance (peak ~ 0.3 V) and 40 % is found in the smaller resonances (< 0.05 V).

One might wonder firstly, whether the measured scattering around the reflected beam is sufficient to explain all power loss in a Fabry-Perot resonator in operation and secondly, whether the reflection and the transmission channel affect each other by scattering. To answer the first question, it is important to note that the power ratio of the scatter around the transmitted and reflected beam equals the ratio of the totally transmitted and reflected power. To appreciate this argument, we mention that the angular distributions in both channels are similar as they are Fourier related to the spatial distribution of the same surface. To answer the second question, we mention that our system produces predominantly small-angle scatter. Light scattered out of the beam transmitted by the mirror will therefore not affect light in the reflected beam (and vice versa) because of the angular difference of almost 180°.

2.4 Connection between cavity finesse and cavity ring-down

In this Section, the performance of a Fabry-Perot is described in terms of the finesse F, which depends on the losses of the resonator via

$$F = \frac{\pi}{1-R} = \frac{\pi}{A+T} \,. \tag{2.7}$$

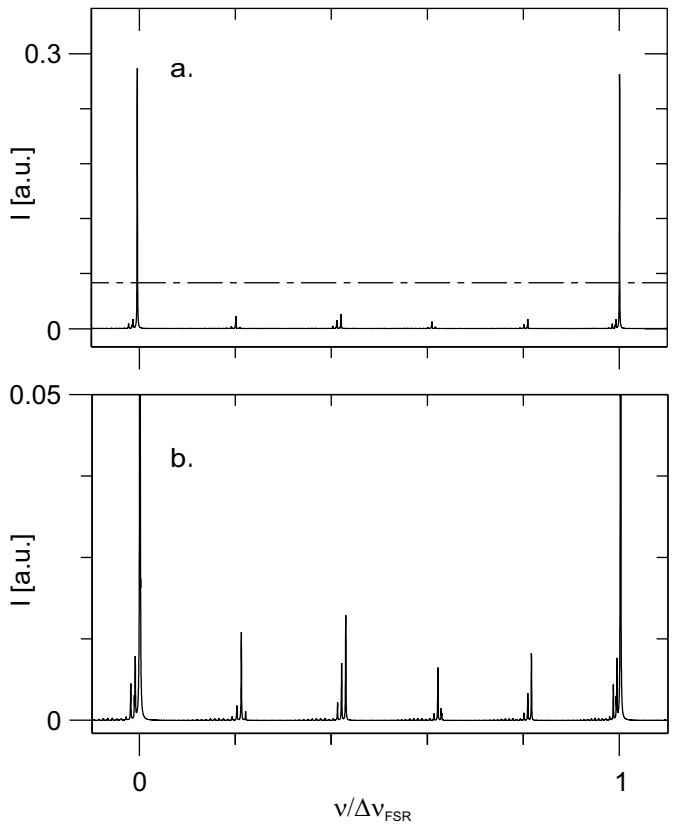

Figure 2.5: *(a) Transmission spectrum of the resonator for one free spectral range. The dashed line indicates the zoomed-in area shown in (b).*

So, if we are able to measure the cavity finesse, the losses can be determined with this relation. Two methods are introduced here, a spectral method and a temporal one.

The spectral method determines the finesse via the ratio of the free spectral range $\Delta\nu_{\mathrm{FSR}}$ and the (FWHM) spectral linewidth $\Delta\nu$

$$F = \frac{\Delta\nu_{\mathrm{FSR}}}{\Delta\nu} \,. \tag{2.8}$$

The temporal method is based on the measurement of the $1/e$ decay time τ of the intracavity intensity after the optical injection has been switched off. This is a so-called "cavity ring-down" experiment [2]. Substitution of the relations $\Delta\nu = 1/(2\pi\tau)$ and $\Delta\nu_{\mathrm{FSR}} = c/(2L)$ into Eq. 2.8 shows how the finesse can also be determined from τ

$$F = \tau\pi c/L \,, \tag{2.9}$$

where c is the speed of light and L is the cavity length.

Performing the spectral measurement, we found that the mirror mounts show a pronounced mechanical resonance at 75 Hz with an acoustic Q-factor of approximately 50. To avoid this resonance, and also its higher harmonics, the scan frequency of the piezo is chosen at 4.6 Hz. At this frequency, the resonator scans in 3.8 ms and 2.8 µs through a FSR and a resonance, respectively. The measured resonance width has a statistical error of 2 %; the line shape is nicely Lorenzian, which shows that the scanning of the resonator is not too fast to perturb the intra cavity field and produce ringing [35]. From this method, we found $F = 1380 \pm 40$. Substituting F in Eq. 2.7 results in $A + T = 2.3 \times 10^{-3}$ which combines with the transmission of a single mirror $T = 4.1 \times 10^{-4}$ to $\eta = (18.0 \pm 0.5)$ %.

Performing the temporal measurement, we start by slowly scanning the resonator length. On the peak of a resonance, a trigger switches off the laser light with an acousto-optic modulator (AOM ISOMET 1205-2). The injection beam switches off in 35 ns and we detect the decaying signal with a 20 MHz-bandwidth detector. The measured decay signal gives a nice exponential decay over two orders of magnitude as shown in Fig. 2.6. The $1/e$ decay time found is $\tau = 0.18$ µs which, in combination with Eq. 2.9, results in $F = 1700 \pm 40$. Furthermore, $A + T = 1.84 \times 10^{-3}$, found from Eq. 2.7, combined with the transmission of a single mirror $T = 4.1 \times 10^{-4}$, gives a cavity efficiency $\eta = (22.2 \pm 0.5)\%$.

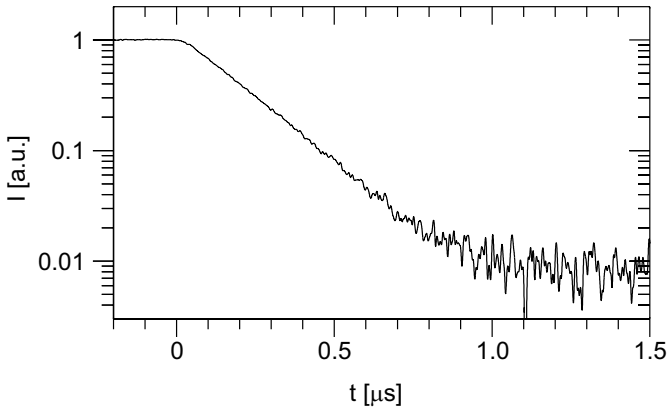

Figure 2.6: *Ring-down curve of a resonator with a cavity length $L = 0.1$ m. The light is switched off at $t = 0$ µs. The fitted ring-down time $\tau = 0.18$ µs corresponds to a finesse of $F = 1700$.*

The difference between the finesse measured with the spectral method and cavity ring-down may be surprising, but has been observed before. A possible explanation has been given by Rempe *et al.* [16]. They state that for a proper *spectral* measurement spatial coherence of the injected field should be retained after repeated reflections. A *temporal* ring-down experiment, however, only requires energy confinement within the cavity, which imposes only a restriction on the "incoherent" field. This is less critical to perturbations by, *e.g.*, scatter, than the restriction on the coherence of the field. Loosely speaking, one might say (in solid-state terminology) that spectral measurements yield something like a T_2-time, whereas temporal measurements yield a T_1-time.

The ring-down method offers an independent method to reject the "trapped-light hypoth-

esis" introduced above. Light recycled in other transverse modes would effectively enlarge the ring-down time. Experimentally, the trapping of scattered light in lower-order modes can be excluded by inserting an intracavity pinhole, absorbing the scattered light. The diameter is chosen such that the lowest order mode is left unaffected. Doing so, the ring-down time of the resonator with intra-cavity pinhole should be shorter than for the situation without. However, the ring-down times were found to be independent of the presence of the intracavity pinhole, consistent with our results in the spectral domain. Apparently, the proper argument is that only a single mode is resonant and scatter cannot be trapped in other modes as they are not resonant. The difference between both methods thus remains unsolved.

2.5 Concluding discussion

The roughness-induced scatter limits the performance of a Fabry-Perot. The scatter of a single mirror is visualized and described by the BRDF and TIS and compared with the losses of a resonator, comprising two mirrors. We show that the finesse and the peak throughput are lower than expected from the mirror's transmission. We have quantified the resonator

Method	Efficiency (η)
TIS	20 %
incoherent illumination	(23.6 ± 0.1) %
coherent illumination	(20 ± 2) %
F_{spectral}	(18.0 ± 0.5) %
$F_{\text{ring-down}}$	(22.2 ± 0.5) %

Table 2.1: *An overview of the resonator efficiency η determined by the various methods in this Chapter: Via angular-resolved scatter of a single mirror (TIS), via average power measurements for incoherent and coherent illumination of a resonator, and via the spectral width and cavity ring-down.*

efficiency $\eta = T/(A+T)$ by various methods as shown in Tab. 2.1. It shows that all methods give roughly (within statistical errors) identical results; the efficiency of the resonator under study being $\eta \approx 20$ %. Thus 80 % of the light escapes via roughness-induced scattering of both mirrors. Furthermore both the "floor" of a spectrum and the comparison of a spectral and temporal method demonstrate that the scattered light is not resonantly trapped inside the resonator.